Eur Biophys J (2011) 40:1101–1107
DOI 10.1007/s00249-011-0719-y

BIOPHYSICS LETTER

Secondary structure determination by FTIR of an archaeal ubiquitin-like polypeptide from *Natrialba magadii*

M. V. Ordóñez · J. Guillén · D. Nercessian · J. Villalaín · R. D. Conde

Received: 21 March 2011 / Revised: 27 May 2011 / Accepted: 1 June 2011 / Published online: 24 June 2011

Abstract The ubiquitin protein belongs to the β-grasp fold family, characterized by four or five β-sheets with a single α-helical middle region. Ubiquitin-like proteins (Ubls) are structural homologues with low sequence identity to ubiquitin and are widespread among both eukaryotes and prokaryotes. We previously demonstrated by bioinformatics that P400, a polypeptide from the haloalkaliphilic archaeon *Natrialba magadii*, has structural homology with both ubiquitin and Ubls. This work examines the secondary structure of P400 by Fourier transform infrared spectroscopy (FTIR). After expression in *Escherichia coli*, recombinant P400 (rP400) was separated by PAGE and eluted pure from zinc-imidazole reversely stained gels. The requirement of high salt concentration of this polypeptide to be folded was corroborated by intrinsic fluorescence spectrum. Our results show that fluorescence spectra of rP400 in 1.5 M KCl buffer shifts and decreases after thermal denaturation as well as after chemical treatment. rP400 was lyophilized and rehydrated in buffer containing 1.5 M KCl before both immunochemical and FTIR tests were performed. It was found that rP400 reacts with anti-ubiquitin antibody after rehydration in the presence of high salt concentrations. On the other hand, like ubiquitin and Ubls, the amide I′ band for rP400 shows 10% more of its sequence to be involved in β-sheet structures than in α-helix. These findings suggest that P400 is a structural homologue of the ubiquitin family proteins.

Keywords Halophilic archaea · *Natrialba magadii* · Ubiquitin-like proteins · β-grasp fold · FTIR · Structural homology

M. V. Ordóñez (✉) · D. Nercessian · R. D. Conde
Instituto de Investigaciones Biológicas,
Facultad de Ciencias Exactas y Naturales,
Universidad Nacional de Mar del Plata, CONICET,
CC: 1245, 7600 Mar del Plata, Argentina
e-mail: mvordone@mdp.edu.ar

J. Guillén
Departamento de Bioquímica y Biología Molecular A,
Universidad de Murcia, Espinardo-Murcia, Spain

J. Villalaín
Instituto de Biología Molecular y Celular,
Universidad Miguel Hernández, Elche-Alicante, Spain

Introduction

Archaea are classified as the third domain of life because they are significantly distinct from Bacteria and Eukarya (Woese et al. 1990). Most archaeal microorganisms are adapted to live under extreme environmental conditions (Brown and Doolittle 1997). Among them, Halobacteriaceae is a family whose members need high NaCl (>3 M) concentrations for growth (Kamekura and Kates 1997). In recent years many archaeal proteins have been characterized. These records suggest that archaeal proteins associated with energetic metabolism and genetic information are often related to their bacterial and eukaryal counterparts, respectively (Brown and Doolittle 1997). Because of these similarities, and despite the absence of already sequenced archaeal genomes, whether archaea have a conjugative system of proteins like the eukaryal ubiquitin pathway has been analyzed (Bienkowska et al. 2003).

Ubiquitin is a highly conserved protein within the eukaryotic domain that was first described as a modifier that attachs to proteins allowing them to be recognized and degraded by the 26S proteasome (Ciechanover 1994). Thus far, ubiquitin has been shown to play several cellular roles, from proteolysis to DNA repair and protein trafficking

(Ciechanover and Iwai 2004; Hochstrasser 2009). Despite being widespread among eukaryotes, ubiquitin is not present in prokaryotes. However, several proteins known as ubiquitin-like (Ubl) and ubiquitin-like domain (UbD) proteins have been identified in the three domains of life (Hartmann-Petersen and Gordon 2004; Hochstrasser 2009; Humbard et al. 2010). These proteins display the conserved β-grasp fold characteristic of ubiquitin and, usually, low amino acid sequence identity with ubiquitin (Iyer et al. 2006). This fold comprising four or five β-sheet strands with a helical segment between the second and third strand has been found to be the scaffold for a diverse set of functions among all organisms (Burroughs et al. 2007).

Ubiquitin-like proteins not only share a 3D structure homology with ubiquitin but also conjugate to target proteins like ubiquitin does (Hochstrasser 2009). Among prokaryotes, ThiS and MoaD are the most studied Ubls. These proteins are involved in the biosynthetic pathway of cofactors thiamine and molybdenum (Marquet 2001; Rudolph et al. 2001; Wang et al. 2001). They display a similar mechanism to the ubiquitin conjugation pathway and are described as functional homologues of ubiquitin (Hochstrasser 2000; Iyer et al. 2006). Recently, Humbard et al. (2010) described the presence of two ubiquitin-like small archaeal modifiers (SAMP1 and SAMP2) from *Haloferax volcanii* that bind cellular proteins similarly to ubiquitin and Ubls. The physiological role of these conjugates is not yet known. At the same time, ubiquitin-like domains are present in one or several repeats close to either the N- or C-terminus of large nonconjugable proteins (Hartmann-Petersen and Gordon 2004). These proteins have been mainly described in eukaryotes and form a more functionally diverse group than Ubls (Burroughs et al. 2007; Grabbe and Dikic 2009).

Previously, by *in silico* analysis, we showed that a polypeptide of 124 amino acids named P400 from the haloalkaliphilic archaeon *Natrialba magadii* has high 3D structural homology with ubiquitin (Nercessian et al. 2009). In addition, we found that P400 expressed in *Escherichia coli* and refolded in a high concentration of KCl reacts with anti-ubiquitin antibody. From these results, we inferred that P400 could be described as a ubiquitin-like polypeptide (Nercessian et al. 2009). This could indicate that *N. magadii* as well as other archaea contain proteins representing the ancestors of the eukaryotic ubiquitin.

When attempting to identify new Ubls and UbDs, both the secondary and tertiary structure of candidates must be determined. Halophilic proteins usually require high salt concentration in the medium to keep their native fold (Eisenberg et al. 1992; Madern et al. 2000), which complicates their structural analysis. Thus, vibrational spectroscopies, such as Fourier transform infrared spectroscopy (FTIR) and circular dichroism (CD), are important and commonly used techniques for protein structure studies (Barth 2007; Haris and Severcan 1999; Severcan et al. 2001).

As part of the current work performed to characterize P400, we have determined its structural parts by FTIR analysis. We also performed intrinsic fluorescence analysis of the polypeptide and corroborated its folded state at high salt concentrations. For this, a little used protein purification technique was adapted to obtain high amounts of pure P400.

Materials and methods

Biological material and growth media

Escherichia coli Rosetta (DE3) cells were grown in LB medium at 37°C under aerobic conditions and constant agitation (170 rpm). Growth was measured by optical density at 600 nm (OD600).

Heterologous expression and purification of P400 polypeptide

Expression of *p400* DNA fragment in *E. coli* Rosetta cells was performed as previously described (Nercessian et al. 2009). Purification by affinity chromatography to Ni^{2+} of the recombinant polypeptide present in the inclusion bodies gave a low yield of purified protein (data not shown). Then, Rosetta cells containing the construction *pET24b-p400* induced with 0.5 mM of IPTG for 3 h were harvested. The cell pellet was sonicated in buffer Tris-HCl 100 mM pH 8—0.5 M NaCl and centrifuged at 17,000×*g* for 30 min. The insoluble fraction was resuspended in sample buffer containing 8 M urea and 1 mM DTT and incubated for 16 h at 25°C followed by 10 min at 37°C. Then, this sample was subjected to SDS-PAGE as described by Laemmli (1970). Protein bands were revealed by means of the Zn-imidazole staining protocol described by Hardy and Castellanos-Serra (2004). Pictures of gels were taken by scanning against a black background. The recombinant P400 (rP400) band (RM: 23 kDa) was cut and eluted from the gel with 30 mM Tris-50 mM glycine pH 8 and lyophilized after dialysis against distilled water.

Refolding of P400 and Western blot tests

Protein concentration was determined by the bicinchoninic acid method (Smith et al. 1987) using bovine serum albumin as standard. Refolding of purified rP400 in solution was performed as described before (Nercessian et al. 2009). In addition, to verify the refolding of the lyophilized rP400 used in the FTIR assays, this was resuspended in buffer

Tris-HCl 100 mM pH 8 with KCl 1.5 M and incubated at 18°C for 16 h. The different preparations of purified rP400 (4 μg) were loaded on polyacrylamide gel (12%). For this, SDS-PAGE was carried out under nonreducing conditions and without boiling the samples. Ubiquitin (1 μg) and trypsin inhibitor (1 μg) were used as positive and negative controls, respectively, of the Western blot test. After electrophoresis, the separated proteins were transferred to nitrocellulose membranes and subjected to Western blotting using 1:100 rabbit anti-ubiquitin primary antibody (Sigma) performed as described by Nercessian et al. (2009).

Fluorescence tests

Chemical denaturations were carried out by adding the corresponding amount from an 8 M stock solution of GdmCl. Changes with increasing concentrations of GdmCl were followed by variations in the maximum fluorescence intensity and in the emission maximum wavelength. Samples of rP400 were excited at 280 nm, and spectra were recorded between 300 and 400 nm. Measurements were carried out in a 1 cm quartz cuvette with rP400 solubilized in a buffer containing 100 mM HEPES, 1.5 M KCl, pH 8.0. Intensity values were corrected for dilution, and subtraction of background emission contribution was derived from GdmCl titration of a buffer blank. Thermal denaturation of rP400 was monitored by a decrease in fluorescence intensity in a Varian Cary Eclipse spectrofluorometer with excitation and emission of 280 and 350 nm, respectively, and 4 nm spectral bandwidths [thermal denaturation curves at excitation 295 nm yielded similar results (see "Results")].

Infrared spectroscopy (IR)

For the infrared measurements, lyophilized rP400 polypeptide was resuspended in 25 μl D_2O buffer 100 mM HEPES containing 1.5 M KCl to a final concentration of 16 mg/ml. The sample in solution was incubated at 18°C for 16 h. The refolded polypeptide was placed between two CaF_2 windows separated by 56 μm thick Teflon spacers and transferred to a Harrick Ossining demountable cell. Fourier transform infrared spectra were obtained in a Bruker IFS55 Fourier transform infrared spectrometer equipped with a deuterated triglycine sulfate detector. Each spectrum was obtained by collecting 500 interferograms with a nominal resolution of 2 cm^{-1}, which were transformed using triangular apodization. To average background spectra between sample spectra over the same time period, a sample shuttle accessory was used to obtain sample and background spectra. The spectrometer was continuously purged with dry air at a dew point of −40°C to remove atmospheric water vapor from the bands of interest. Band-narrowing strategies were applied to resolve the component bands in the amide I′ region. Second-derivative spectra were calculated over a 15-data point range. Fourier self-deconvolution (Kauppinen et al. 1981) of the subtracted spectra was carried out using a Lorentzian shape and a triangular apodization with a resolution enhancement parameter, *K*, of 2.2, which is lower than log (signal/noise) (Mantsch et al. 1988) and a full width at half-height of 18 cm^{-1}. These parameters assumed that the spectra were not overdeconvolved as was evidenced by the absence of negative side lobes. Protein secondary structure elements were quantified from curve-fitting analysis by band decomposition of the original amide I′ band after spectral smoothing using the same software stated above (Palomares-Jerez et al. 2010). Briefly, for each component, three parameters were considered: band position, band height, and band width. The number and position of component bands was obtained through deconvolution, and in decomposing the amide I′ band, Gaussian components were used. The curve-fitting procedure was accomplished in two steps: in the first one, band position was fixed, allowing widths and heights to approach final values, and in the second one, band positions were left to change. Band decomposition was performed using SpectraCalc (Galactic Industries). The fitting result was evaluated visually by overlapping the reconstituted overall curve on the original spectrum and by examining the residual obtained by subtracting the fitting from the original curve. The procedure gave differences of less than 2% in band areas after the artificial spectra were submitted to the curve fitting procedure.

Results and discussion

Purification and refolding of P400 polypeptide

Previously using Ni^{2+} affinity chromatography, we isolated the recombinant P400 polypeptide (rP400) to 90% purity (Nercessian et al. 2009). However, this procedure was not suitable to obtain rP400 for FTIR because this technique requires high amounts of entirely pure samples. Consequently, we subjected *E. coli* inclusion bodies holding rP400 to SDS-PAGE followed by reverse staining of gel with zinc-imidazole as described by Hardy and Castellanos-Serra (2004). This infrequently used technique is based on the zinc imidazolate selective precipitation in the gel parts not containing protein. Thus, throughout these steps, pure rP400 was eluted from the gel with a 90% yield (Fig. 1).

Because dehydration can irreversibly change the secondary structure of proteins (Griebnow and Klibanov 1995; Prestrelski et al. 1993), its effect on pure rP400 was examined. Figure 2 shows that rP400 refolded by dialysis against buffer with 1.5 M KCl reacts with the anti-ubiquitin

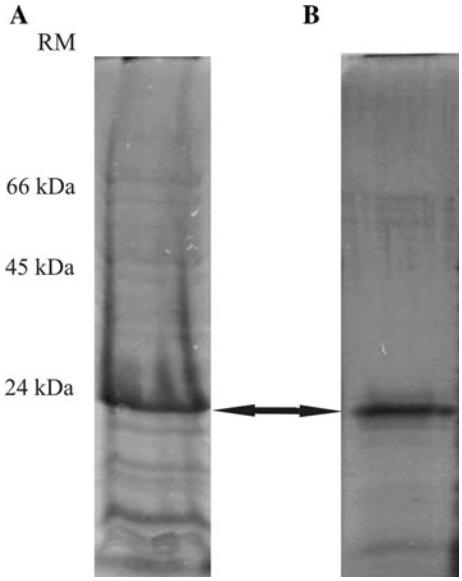

Fig. 1a, b Purification of recombinant P400 polypeptide by elution from zinc-imidazole reverse stained polyacrylamide gels. **a** 12% polyacrylamide SDS-PAGE of insoluble fraction of *E. coli* Rosetta strain cells induced with IPTG over 3 h. **b** 12% polyacrylamide SDS-PAGE of purified rP400 polypeptide from gel **a**. The band corresponding to rP400 in gel **a** was excised and the protein was eluted from the gel as described (for details see "Materials and methods"). *RM* (relative mass) indicates the position of the molecular weight standards. *Black arrow* indicates the band corresponding to rP400 polypeptide

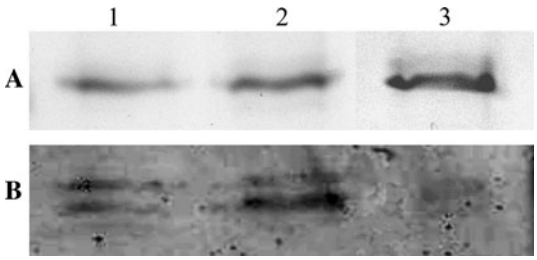

Fig. 2a, b Immunodetection of recombinant P400 polypeptide with anti-ubiquitin antibody. **a** Nonreducing 12% polyacrylamide SDS-PAGE. **b** Western blot assay of purified rP400 using anti-ubiquitin antibody (for details see "Materials and methods"). *Lane 1* rP400 purified, lyophilized, and resolubilized in buffer containing 1.5 M KCl, *lane 2* rP400 purified and dialized against buffer with 1.5 M KCl, *lane 3* purified rP400 in elution buffer (30 mM Tris-50 mM glycine). Equal amounts of proteins were loaded

antibody. Also, it shows that this reaction is similar for the lyophilized rP400 rehydrated in the same buffer. As can be seen from the figure, the antibody reacts with 2 min bands at the rP400 region. The possibility that these bands are different folding forms of rP400 separated in semi-denaturing condition should not be discarded. Also, owing to the requirement of salt for refolding, only a small amount of protein is detected by the antibody when rP400 is rehydrated in nonsaline solution (Fig. 2, lane 3). It may be also noted that similar results to those shown in Fig. 2 are seen by dot blot tests (data not shown). All of these results demonstrate that lyophilization of the purified rP400 does not impede its refolding when rehydrated in buffer with 1.5 M KCl for FTIR tests. In other words, the results support the idea that conformational changes induced by lyophilization could be reversed depending on the structure of each protein (Luthra et al. 2006; Prestrelski et al. 1993). Indeed, while lyophilization of β, α, and disordered proteins has been shown to induce partially irreversible changes, most α/β proteins recover their original conformation after rehydration (Prestrelski et al. 1993), which agrees with the present characterization of rP400.

Fluorescence tests

The fluorescence spectra of the polypeptide in buffer with 1.5 M KCl and with the denaturating agent 5 M guanidine hydrochloride are shown in Fig. 3a. P400 has a sole tryptophan at position 71 and four tyrosines at positions 8, 13, 48, and 109 (Fig. 3d). At an excitation wavelength of λ_{exc} = 280 nm, the emission fluorescence spectrum is red shifted, to a maximum at 349 nm (Fig. 3a, continuous line). This indicates that the tryptophan is in a polar environment partially solvent-exposed. This fact would agree with the proposed model of the 3D structure (Fig. 3d), with the Trp exposed in a loop of the structure. In the presence of GdmCl, the fluorescence intensity decreased and the emission maximum wavelength was shifted (Fig. 3a, dotted line). As shown by the chemical denaturation curve (Fig. 3b), rP400 readily denatures as the concentration of denaturant ranges between ~2 and 3.5 M GdmCl, with a $[GdmCl]_{50\%}$ of 2.9 M. These results were further corroborated by the red-shift displacement in the emission frequency maximum (Fig. 3a).

To further investigate the structural stability of rP400, thermal denaturation was monitored through the decrease in intrinsic fluorescence as the temperature increased (Fig. 3c). The fluorescence intensity did not change in a perfect sigmoidal fashion typical of a cooperative process, but this fact could be due to the solvent-exposed situation of the Trp in the protein. The thermal denaturation of rP400 was irreversible as shown in the rescanning curve. Tests with excitation at 295 nm were performed to gain information on the Trp and Tyr residue contributions to the fluorescence spectra. Both spectra and thermal denaturation curves at excitation wavelengths of 280 and 295 nm showed similar results, suggesting a main contribution of Trp71.

Secondary structure of P400

To confirm whether the rP400 polypeptide from *N. magadii* adopts the previously predicted shape, its secondary structure components were assessed by FTIR (Fig. 4). The broad

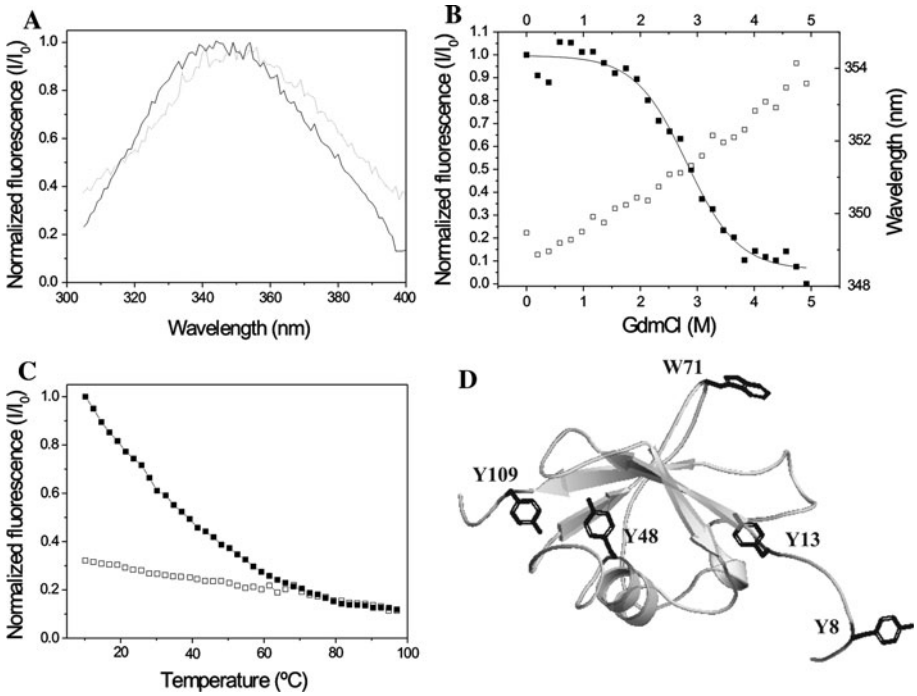

Fig. 3a–d Analysis of recombinant P400 folding state under high salt concentration by intrinsic fluorescence measurements. Effect of the denaturing agent guanidine hydrochloride on the shift of the emission maximum wavelength and fluorescence intensity. **a** Normalized fluorescence spectra of rP400 in HEPES 100 mM and 1.5 M KCl and in 5 M of GdmCl. **b** Changes in wavelength (*right axis, filled squares*) and in normalized fluorescence intensity (*left axis, open squares*) upon increasing GdmCl concentration. The data were fit by a simple sigmoid. **c** Thermal denaturation followed by intrinsic fluorescence. The experimental trace shows the normalized changes in the fluorescence emission at 350 nm upon excitation at 280 nm, as the temperature is increased (*filled squares*) and the normalized fluorescence of the rescanning as the temperature is decreased (*open squares*). **d** Ribbon representation of P400 3D structure model. The tyrosine (*Y*) and tryptophan (*W*) residues contained in the polypeptide are represented and highlighted in *black*. The *numbers* indicate the position of the residue in P400 sequence. Modified from Nercessian et al. (2009)

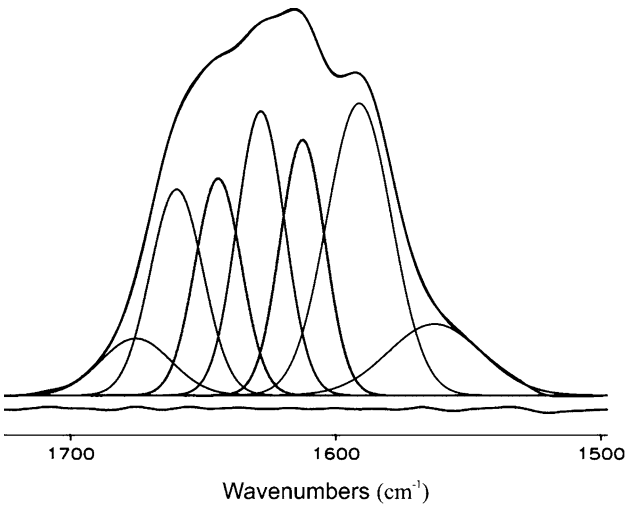

Fig. 4 Fourier transformed infrared spectroscopy of recombinant P400 polypeptide from *Natrialba magadii*. Amide I′ band decomposition of the spectra of rP400 protein in solution containing 1.5 M KCl. The component bands, the original envelope, and the difference between the fitted curve and the original spectrum are shown

amide I′ band of the IR spectrum of a protein is a consequence of the C=O streching vibrations of the peptide backbone. The frequencies of the amide I′ band components are closely correlated to each secondary structural element in the proteins (Barth 2007; Kong and Yu 2007). To observe the underlying components of the broad amide I′ band of the protein, several enhancements methods were applied, such as self-deconvolution and derivative methods, to the original envelope (Kauppinen et al. 1981) as well as decomposition of the amide I′ infrared band. As can be observed in the figure, different component bands with frequencies at 1,675, 1,660, 1,644, 1,628, and 1,612 cm^{-1} were identified. They can be assigned to ß-turn, α-helix, random coil, ß-sheet, and Tyr side chains, respectively (Arrondo and Goni 1999). Table 1 shows the percentages of each structural component in the polypeptide found by fitting (see "Materials and Methods"). It can be observed that the 1,628 cm^{-1} band, corresponding to β-sheet structure, was the main component of the broad amide I′ band (35%). α-Helix and random coil comprise about 29 and 26%, whereas ß-turns comprise about 10% of the protein. Therefore, the main structural component of the protein is β-sheet, followed by α-helical structures and random coils.

According to the data obtained from the X-ray crystallization of human ubiquitin [PDB (Protein Data Bank) name: 1Ubq] this protein is composed of 23% helical structures

Table 1 rP400 amide I′ band secondary structure components

Vibrational frequency (cm^{-1})	Type of structure	Structure (%)
1,675	β-Turn	10
1,660	α-Helix	29
1,644	Random coil	26
1,628	β-Sheet	35

and 34% β-sheet structures (Vijay-Kumar et al. 1987). Data extracted from the amide I′ band of the analyzed protein demonstrate that rP400 has similar percentages of its sequence involved in β-sheet and α-helical structures as ubiquitin. This result is in good agreement with the composition of the β-grasp fold exhibited not only by human ubiquitin but also by all the representatives of the ubiquitin protein family. The fold is characterized by four or five β-strands with a unique α-helix in the middle region of the protein (Burroughs et al. 2007). Our previous report of P400 shows that a homology model could be obtained from the alignment of P400 and the well characterized human ubiquitin (Nercessian et al. 2009). This model displays an arrangement of the structural components along P400 similar to that described for the β-grasp proteins. As can be seen, results obtained by FTIR empirically corroborate the previously predicted secondary structure and 3D model as well as its structural homology with the ubiquitin protein family. Therefore, it could be assumed that P400 polypeptide has a similar structural composition to that of ubiquitin and the β-grasp fold family of proteins.

Conclusion

In this work we present the FTIR analysis of rP400 under native conditions that corroborates previously reported information. According to these results, rP400 exhibits a similar composition of β-sheets and α-helices to ubiquitin and ubiquitin-like proteins from both prokaryotes and eukaryotes (Iyer et al. 2006). We also show that pure rP400 can be prepared by SDS-PAGE of inclusion bodies followed by elution from gels stained with zinc-imidazole. This strategy led us to obtain P400 that was more pure than that obtained by Ni^{2+} affinity chromatography. Finally, lyophilization followed by refolding of rP400 for spectroscopic analysis did not alter its secondary structure, which is also supported by its reactivity with anti-ubiquitin antibody. In this sense, the structural stability of rP400 under high salt concentration was corroborated by fluorescence measurements. Chemical as well as thermal denaturation treatments were performed on the sample, and a decrease in the intrinsic fluorescence and a shift in the maximum emission frequency were observed. It can therefore be concluded that the protein is in a folded state under high salt concentration.

The β-grasp fold is highly conserved among the three domains of life and serves as scaffold for many different biochemical processes (Burroughs et al. 2007; Iyer et al. 2006). Since P400 does not show sequence identity with any known protein, to date no cellular role can be assigned to it. Regardless, given that P400 displays one of the most conserved folds in nature, we believe it could play a key role in cell physiology. In our future work we hope to analyze the complete primary structure, folding features, cellular localization, and biological role of P400-containing protein from *N. magadii*.

Acknowledgments This work was supported by grants PIP 6049 from Consejo Nacional de Investigaciones Científicas y Técnicas (CONICET), Argentina; EXA397/08 from Universidad Nacional de Mar del Plata (UNMdP), Argentina; and BFU2008-02617-BMC from Ministerio de Ciencia y Tecnología, España. Authors are grateful to Dr. Rosana de Castro for contributing materials for the heterologous expression assays. J.G. was the recipient of a postdoctoral fellowship from the Programa Juan de la Cierva Ministerio de Ciencia e Innovación.

References

Arrondo JL, Goni FM (1999) Structure and dynamics of membrane proteins as studied by infrared spectroscopy. Prog Biophys Mol Biol 72:367–405

Barth A (2007) Infrared spectroscopy of proteins. Biochim Biophys Acta 1767:1073–1101

Bienkowska JR, Hartman H, Smith TF (2003) A search method for homologs of small proteins. Ubiquitin-like proteins in prokaryotic cells? Protein Eng 16(12):897–904

Brown JR, Doolittle WF (1997) Archaea and the prokaryote-to-eukaryote transition. Microbiol Mol Biol Rev 61(4):456–502

Burroughs AM, Balaji S, Iyer LM, Aravind L (2007) Small but versatile: the extraordinary functional and structural diversity of the beta-grasp fold. Biol Direct 2:18. doi:10.1186/1745-6150-2-18

Ciechanover A (1994) The ubiquitin-proteasome proteolytic pathway. Cell 79(1):13–21

Ciechanover A, Iwai K (2004) The ubiquitin system: from basic mechanisms to the patient bed. IUBMB Life 56(4):193–201

Eisenberg H, Mevarech M, Zaccai G (1992) Biochemical, structural, and molecular genetic aspects of halophilism. Adv Protein Chem 43:1–62

Grabbe C, Dikic I (2009) Functional roles of ubiquitin-like domain (ULD) and ubiquitin-binding domain (UBD) containing proteins. Chem Rev 109(4):1481–1494

Griebnow K, Klibanov AM (1995) Lyophilization-induced reversible changes in the secondary structure of proteins. Biochemistry 92:10969–10976

Hardy E, Castellanos-Serra LR (2004) Reverse-staining of biomolecules in electrophoresis gels: analytical and micropreparative applications. Anal Biochem 328:1–13

Haris PI, Severcan F (1999) FTIR spectroscopic characterization of protein structure in aqueous and non-aqueous media. J Mol Catal B Enzym 7:207–221

Hartmann-Petersen R, Gordon C (2004) Integral UBL domain proteins: a family of proteasome interacting proteins. Semin Cell Dev Biol 15(2):247–259

Hochstrasser M (2000) Evolution and function of ubiquitin-like protein-conjugation systems. Nat Cell Biol 2(8):E153–E157

Hochstrasser M (2009) Origin and function of ubiquitin-like proteins. Nature 458(7237):422–429

Humbard MA, Miranda HV, Lim J, Krause DJ, Pritz JR, Zhou G, Chen S, Wells L, Maupin-Furlow JA (2010) Ubiquitin-like small archaeal modifier proteins (SAMPs) in Haloferax volcanii. Nature 463:54–60

Iyer LM, Burroughs AM, Aravind L (2006) The prokaryotic antecedents of the ubiquitin-signaling system and the early evolution of ubiquitin-like beta-grasp domains. Genome Biol 7(7):R60. doi:10.1186/gb-2006-7-7-r60

Kamekura M, Kates M (1997) Evolution of Archaea: a view of halobacteriologists. Viva Orig 25:149–158

Kauppinen JR, Moffatt DJ, Mantsch HH, Cameron DG (1981) Fourier self-deconvolution: a method for resolving intrinsically overlapped bands. Appl Spectrosc 35:271–276

Kong J, Yu S (2007) Fourier transform infrared spectroscopy analysis of protein secondary structure. Acta Biochim Biophys Sin 39(8):549–559

Laemmli UK (1970) Cleavage of structural proteins during the assembly of the head of bacteriophage T4. Nature 227(5259):680–685

Luthra S, Kalonia DS, Pikal MJ (2006) Effect of hydration on the secondary structure of lyophilized proteins as measured by Fourier transform infrared (FTIR) spectroscopy. Biotechnology 96:2910–2921

Madern D, Ebel C, Zaccai G (2000) Halophilic adaptation of enzymes. Extremophiles 4:91–98

Mantsch HH, Moffatt DJ, Casal H (1988) Fourier transform methods for spectral resolution enhancement. J Mol Struct 173:285–298

Marquet A (2001) Enzymology of carbon-sulfur bond formation. Curr Opin Chem Biol 5(5):541–549

Nercessian D, Marino Buslje C, Ordóñez MV, De Castro RE, Conde RD (2009) Presence of structural homologs of ubiquitin in haloalkaliphilic Archaea. Int Microbiol 12:167–173

Palomares-Jerez MF, Guillén J, Villalaín J (2010) Interaction of the N-terminal segment of HCV protein NS5A with model membranes. Biochim Biophys Acta 1798(6):1212–1224

Prestrelski SJ, Tedeschi N, Arakawa T, Carpenter J (1993) Dehydration-induced conformational transitions in proteins and their inhibition by stabilizers. Biophys J 64:661–671

Rudolph MJ, Wuebbens MM, Rajagopalan KV, Schindelin H (2001) Crystal structure of molybdopterin synthase and its evolutionary relationship to ubiquitin activation. Nat Struct Biol 8:42–46

Severcan M, Severcan F, Haris PI (2001) Estimation of protein secondary structure from FTIR spectra using neural networks. J Mol Struct 565–566:383–387

Smith PK, Krohn RI, Hermanson GT, Mallia AK, Gartner FH, Provenzano MD, Fujimoto EK, Goeke NM, Olson BJ, Klenk DC (1987) Measurment of proteins using bicinchoninic acid. Anal Biochem 150:76–85

Vijay-Kumar S, Bugg CE, Cook WJ (1987) Structure of ubiquitin refined at 1.8 A resolution. J Mol Biol 194:531–544

Wang C, Xi J, Begley TP, Nicholson LK (2001) Solution structure of ThiS and implications for the evolutionary roots of ubiquitin. Nat Struct Biol 8:47–51

Woese CR, Kandler O, Wheelis ML (1990) Towards a natural system of organisms: proposal for the domains Archaea, Bacteria and Eukarya. PNAS 87:4576–4579